Twin Telescope observations of the Sun at Kodaikanal Observatory

Jagdev Singh* and B. Ravindra

Indian Institute of Astrophysics, Koramangala, Bangalore 560 034, India

Abstract. We report the design, fabrication and installation of a 'Twin Telescope' at Kodaikanal Observatory intended to augment the ongoing synoptic observations of the Sun that have been carried out since 1904. The telescope uses a 15 cm objective capable of taking Ca-K line filtergrams and photoheliograms in continuum of the full disk of the Sun simultaneously, at a frequency of 0.1 Hz using 2k×2k format CCD cameras. The telescope has been in operation since February 2008 and images are being obtained at a cadence of 5 min during normal observing periods. In case of solar activity, images of the active regions can be taken at a frequency of 1 Hz by restricting the field of view and spatial resolution. In this paper, we describe the telescope, instruments, image acquisition, data calibration and image processing. We also discussed a method of determining the network element and plage area index. The preliminary results show that while the network element covers about 30% of the disk, the percentage of the network element area index varies marginally with the seeing conditions during the day.

Keywords : telescopes – Sun: faculae, plages – Sun: general – Sun: activity

1. Introduction

It is now well known that Sun's ever-changing magnetic field affects the solar irradiance variability on long time scales (Harvey & White 1999) and space weather on short time scales (Srivastava et al. 2009). Long-term regular observations of the Sun are needed to understand the solar activities. At Kodaikanal observatory we have been acquiring daily photoheliograms of the Sun since 1904 using a 15-cm aperture telescope. The observations of Ca-K line were started in 1907 and

---

*e-mail: jsingh@iiap.res.in

H-alpha in 1912. A variety of scientific work have been carried out from the synoptic observations of the Sun. Singh & Bappu (1981) used Ca-K line spectroheliograms to study the variation of network size with the phase of the solar cycle; Singh & Prabhu (1985) found semi-periodic variations in the chromospheric rotation rate with a period of 2, 7 and 11 years. Sunspot data from broad-band images of the Sun obtained since 1904 have been used extensively to study the solar rotation and related topics by a group led by Sivaraman et al. (1999, 2007) and Howard et al. (2000). H-alpha images obtained daily since 1912 have been used by Makarov & Sivaraman (1989), and Makarov, Tlatov & Sivaraman (2001, 2003) for solar cycle studies and its evolution. The data have also been used to study solar activity (e.g., Singh & Gupta 1995; Singh, Sakurai & Ichimoto 2001). It is now understood that these uniform and contiguous data sets are extremely valuable for studying the variations of magnetic field on the Sun over the past 100 years. To keep the data sets uniform while acquiring data with a new telescope, it is important to continue to obtain data and generate a series of images from overlapping data from the earlier instrument and the new one.

Earlier, the images of the Sun were recorded on specialized photographic emulsion suitable for this purpose. With the advancement of electronic technology and development of faster and bigger format CCD cameras, the specialized films went out of production. In 1995 we started using a narrow band filter with the old siderostat and CCD camera of 1k×1k format to take Ca-K line filtergrams. These data have the drawback that images rotate over time and have low spatial resolution compared with the earlier data obtained with the spectroheliograph. To overcome this limitation, we designed and fabricated a Twin Telescope to take Ca-K line and continuum images of the Sun. This telescope has been in operation since 2008 at the Kodaikanal Observatory and have been making images during clear skies.

Though the new telescope installed at Kodaikanal obtains both the Ca-K and white light images, the main focus of this paper is on Ca-K 395 nm image data obtained from one of the telescopes. In the following sections of the paper, we describe the instrument used to obtain the synoptic Ca-K data sets, the observational method and calibration techniques adopted to be make it useful for the scientific community. Subsequently, we present a technique to extract the information about the network element area and plage area index using the calibrated data sets. In the end, we summarize the instrument and the preliminary results.

2. Instrument

The Twin Telescope consists of two tubes mounted on a single equatorial mount, one to obtain the white light images and the other for the Ca-K line filtergrams of the Sun (Fig. 1). Each tube is fitted with 15-cm objective lens from Zeiss to take the image of the Sun at different wavelengths. Each lens of focal length 225 cm forms the full disk solar image of size 2.06 cm. For white light images we use a heat rejection filter of size 15-cm with a pass-band centered at 430 nm and bandwidth of 10 nm which is kept in the entrance of the tube. In addition, a Mylar filter with density 5 is kept in-front of the objective lens to cut down the incoming light intensity so as to reduce the heat load in the telescope tube. The Mylar filter used in the Twin Telescope has a

Figure 1. The Twin Telescope observing the Sun at Kodaikanal Observatory.

refractive index similar to that of ambient air. Index matching prevents wavefront degradation and helps retain the desired image quality with the telescope. On the other hand, the neutral density (ND) filter is generally used near the focal plane. Thus it is not made with optical surface quality and may have some aberrations. The large-sized ND filters with optical surface quality have to be custom made and it is expensive. Hence, we opted for a low cost Mylar filter to reduce the intensity and heat load in the telescope.

The telescope which takes the Ca-K image uses a heat rejection filter with a pass band centered at 395 nm and band-width of 10 nm kept in front of the objective lens. In addition, a Mylar filter with density 3.8 is placed in front of the objective lens. More importantly, a narrow band thermally controlled interference filter with a pass band centered at 393.37 nm and band width of 0.12 nm is kept near the focus to get the Ca-K line images. Thus the Ca-K line filtergrams are obtained with spectral pass band of 0.12 nm centered at the line. The pass band remains stable within 0.001 nm as the temperature of the filter is maintained within 0.1°C. The final image size is 2.06 cm with a small variation over the seasons. The image scale is 93″ mm^{-1}. Two CCD cameras, one for the Ca-K line and the other for the broad-band imager permit us to take simultaneous images of the Sun for the chromospheric and photospheric studies in case of active events on the Sun.

2.1 CCD detector and image acquisition

The CCD cameras having scientific grade-I chip and 2k×2k pixel format with a 16-bit read out at 1 MHz made by Andor provides uniform images with high dynamic range and high photometric

accuracy. The peltier cooled CCD cameras are operated at –40°C for low dark current and low read out noise. The CCD camera used in imaging has a pixel size of 13.5×13.5 microns providing a spatial resolution of 1.25 arc sec per pixel. The ND filters in front of the objective lens permit us to give sufficient large exposure to avoid the visibility of the shutter pattern in the images of the Sun. The exposure time is chosen in the range between 300 ms and 1 second depending on the sky conditions. During the clear sky the exposure time is generally 200 - 300 ms depending on the time of observations. In the morning, exposure time is larger due to large extinction. Large exposure times are used during the presence of high altitude thin clouds. After the alignment of the telescope, the auto guider indicated that drift in the image is about 2-3 arcsec in one minute. This works out to be 0.015 arcsec during the exposure time of 300 ms which is much less than a pixel size. The read out noise of about 20 counts (standard deviation) determined from the dark images which is about 0.1% of the image count, is much less than the photon noise which is about 170 counts in Ca-K line images. The photon noise is about 0.6% of the image count and thus dominates in the photometry. The low dark count of about 300 affects the dynamic range of the 16-bit CCD camera marginally.

The software program allows us to set the exposure time, rate of image acquisition and cadence for saving the images. The white light image of the Sun itself is used to center the image on the CCD detector. The developed software computes the edges of the solar limb and keeps it fixed at specified locations on the CCD cameras within a few pixels. The sequence continues to be recorded until we interrupt it due to the weather conditions. In principle, sequence of the full disk images of the Sun can be obtained with an interval of 6 sec but we normally take the images of the Sun at an interval of 1 minute to guide the image and save the images at an interval of 5 min to keep the data volume at a manageable level. In future, we plan to save the data every 1 min or better to examine the evolution of solar features at different wavelengths. In case of activity on the Sun such as flares, we plan to obtain the images at an interval of 2 sec by restricting the FOV and binning the CCD chip by 2×2 pixels.

In order to know the orientation of the images on the CCD we off center the image towards the East side on the CCD and obtain a portion of the Sun's image. We then allow the image to drift by stopping the telescope. About 70- 80 seconds after stopping the telescope we take another image. A combination of these two images gives the E-W direction of the Earth. This procedure is repeated once in 15 days depending on the sky conditions. We take flat field images in clear sky conditions, preferably once in 3 days, by keeping a diffuser in front of the objective lens. We also take dark images at regular intervals.

2.2   The data calibration

2.2.1   *Flat fielding*

We attempted a number of ways to take the flat-field images. First, we tried by pointing the telescope away from the Sun towards the eastern, western, northern and southern directions and

taking images of the sky. The varying sky brightness with distance from the Sun created a small gradient in the flat-field image. The average of flat-field images showed a small gradient. Hence, we did not adopt this method. Then we obtained the flat-field image by keeping a diffuser in front of the objective and pointed the telescope to the disk center, but the image again showed a small gradient in different directions. The diffuser scatters the solar disk light in all directions in the telescope and probably causes a gradient in the images. The outer portions of the images of the Sun in Ca-K line do not show any arbitrary variations in the background signal due to change in the sky brightness. Absence of gradients except the limb darkening gradients in the Ca-K line images indicate that observed large spatial scale gradients in the flat-field images are because of the method adopted to take the flat field images. It is, therefore, necessary to remove this effect from the flat-field images. The flat-field correction applied to the Ca-K images of the Sun without making the above mentioned correction to the flat-field images caused distortions in the solar images. There are other methods to compute the flat fielding (e.g., Kuhn, Lin & Loranz 1991) for extended objects. We are planning to use one of these methods in future.

The flat images are obtained with the same telescope setup by keeping a diffuser in front of the telescope objective. The flats are taken once in 3 days and sometimes once in a week depending on the sky conditions. A set of obtained dark and flat images are averaged separately. A second degree polynomial is used to remove the gradient in the averaged flat field image caused by the scattered light in the telescope due to the diffuser. The dark current has been subtracted from flat field image and then normalized the flat image to the maximum value of dark subtracted flat. Later, all the Ca-K images are corrected for the flat fielding.

2.2.2 *Image alignment*

The next step is to find the North-South direction on the solar image for which the following steps have been adopted. (1) Two solar images were obtained by stopping the telescope, one in the eastern direction and other in the western direction as explained in Section 2.1. (2) Wherever the Sun's disk is found in the image, those pixels were assigned a value of 1, so that the image has become now a binary map. (3) These images were added. (4) We then identified the pixels that are having maximum counts after adding the images and made those pixel values equal to 1. The rest of the image is made zero. (5) Slicing the image column wise, we identified the column that has only one pixel and its value is 1. (6) Following the 5th step, we identified the two bright pixels that corresponds to the northern and southern direction of the Earth. (7) Then the p-angle is calculated using the standard solarsoft routine by inserting the date and time of the observations. (8) The final angle for the image rotation is computed by considering the value of p-angle and the E-W direction of the Earth on the image of the Sun obtained using the CCD camera. In many occasions, the obtained solar images are not in the center of the image window. By finding the center of the solar image (by centroid finding method) we calculated the required pixel shift of the solar image center from the center of the image window. Once the image center was identified we then rotated the solar image so that the image North pole is in the upward direction. All these data calibrating softwares are written in Interactive Data Language (IDL) from ITT visual. These
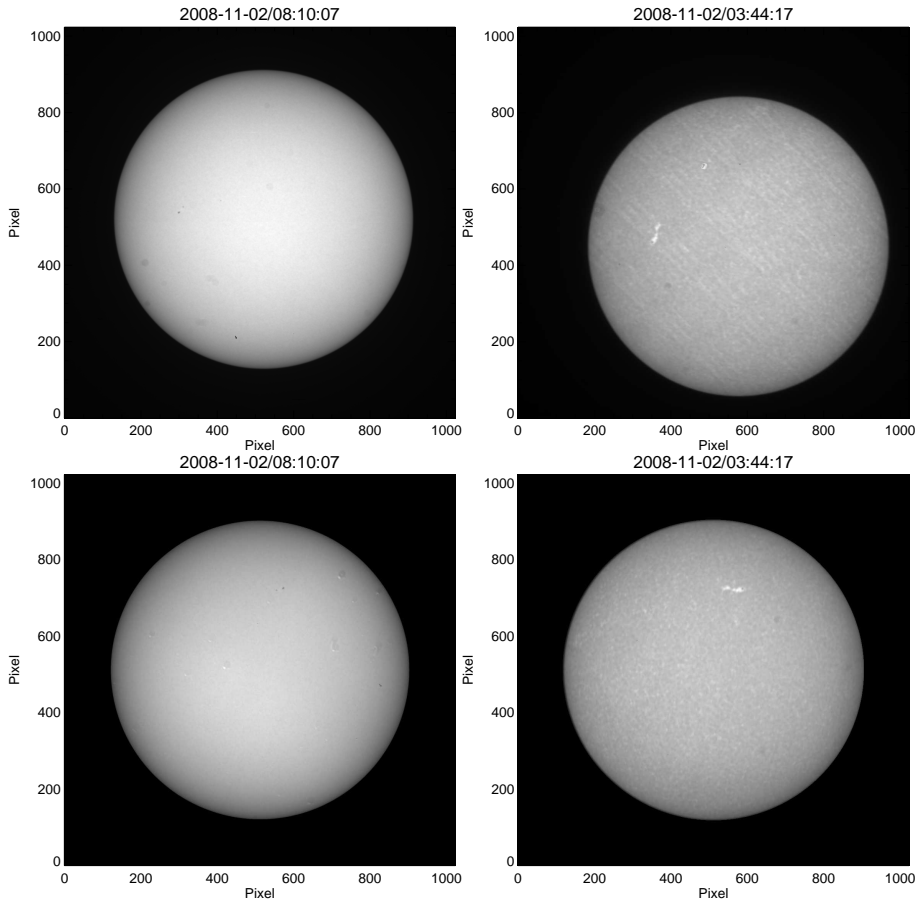
Figure 2. Top left: The raw white light image. Top right: The raw Ca-K image. Bottom right: A preliminary calibrated white light image. Bottom right: A Ca-K image which is flat fielded and rotated to make the North polarity up. The date and time (in UT) of the observations are shown on the top of each image.

calibrated images are then stored in 32 bit FITS format for scientific analysis and also in jpeg image format for a quick look.

2.2.3 *Observations*

The Twin Telescope was made functional on February 23, 2008 and has been obtaining the Ca-K line and white light images of the Sun whenever the sky is clear. The quality of Ca-K data is mostly homogeneous. When the sky is clear the data is acquired once every 5 min. Under clear-sky conditions we are able to get upto 80 images, and upto 10 images on other days. The

telescope is operational and continues to acquire data. Fig. 2(top) shows the typical raw white light (left) and Ca-K (right) images obtained from the Twin Telescope. Fig. 2(bottom) shows the corresponding images that are flat fielded and corrected for the North-South. In raw white-light images, dust particles and non-solar features are clearly visible. These features are largely diminished in the flat-fielded images. The fringe pattern seen in raw Ca-K images has been successfully removed after the flat fielding. However, a few dust particles and other features are still present but these remaining features do not affect the statistical studies.

3. Image processing

The Ca-K images show the well known limb darkening effect. In order to extract any features on the Sun by automatic detection processes it is essential to remove the limb darkening gradient. In the following we describe a method to compute the limb darkening profile and make the required correction.

3.1 Disk center and radius

For many scientific data analysis it is essential to identify the center and radius of the solar disk in the calibrated image. This has been achieved by identifying the solar limb. Solar limb has a steep gradient between the solar disk and the surrounding area. We used the sobel filter to detect the edge of the solar limb. We then used a threshold value of five times the mean value of the sobel filtered image to detect the edges automatically. We assigned a value of one to the limb and kept the rest of the image at zero value. We first sliced the image in the column direction. Since the images are already rotated to make the North pole in the vertical direction, the column first detected on the limb with values equal to one is identified as the East limb of the Sun. Similarly, the last one is taken as the West limb. We then sliced the image in the row direction. Similar as above the first detected limb with values equal to one is taken as the South and the last is taken as the North position of the limb. To detect more points on the limb we have generated circles centered at four corners of the image window. We allowed the circle to grow. Wherever it touched the Sun's limb first is taken as the S-E, N-E, N-W and S-W points. Using the eight detected points on the solar limb we used a polynomial fitting (FIT_CIRCLE.PRO available in the solarsoft) to obtain the Sun center and radius in terms of pixels. With the adoption of this method we could identify the Sun center and radius.

3.2 Removal of limb darkening

The photospheric and chromospheric limb darkening is a gradual decrease in the intensity from disk center to the limb. In order to remove this systematic variations of intensity we followed the method described in Denker et al. (1999). Following this method, we first computed a median intensity in a small box enclosing the disk center. The data is transformed to polar co-ordinates
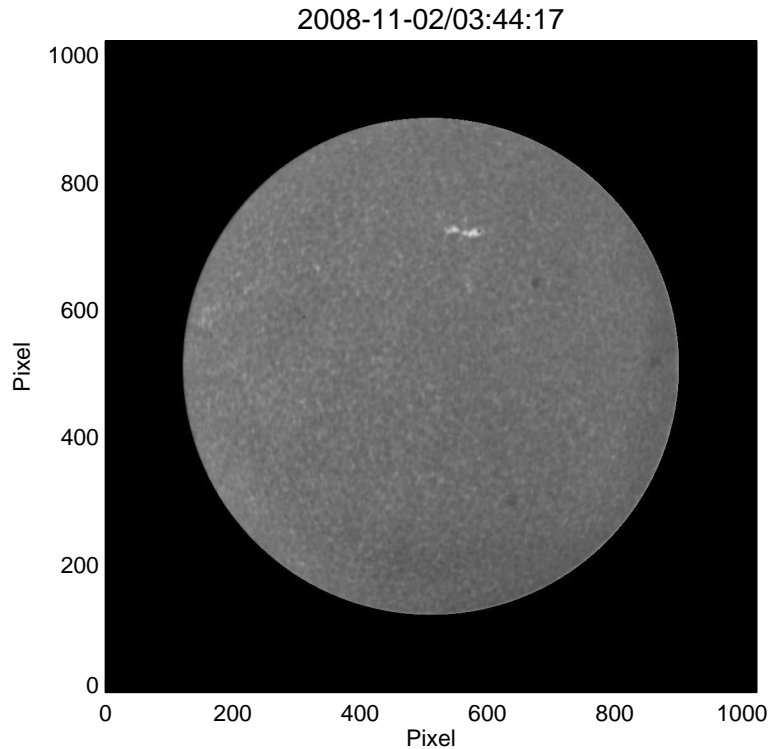
2008-11-02/03:44:17

Figure 3. The limb darkening corrected Ca-K image corresponding to Fig. 2 (bottom right).

that resulted in one radial profile for every 1° azimuth. A median value is obtained at each radial position to get the average radial profile. The inner portion of the average disk profile is replaced with a second order polynomial fit to the average radial profile. Once again the average disk profile is smoothed by large smoothing kernels. The resulting smoothed profile is transformed to the Cartesian co-ordinate system. The pixels outside the disk are replaced with zeros. A typical limb darkening corrected image is shown in Fig. 3.

3.3 Removal of residual gradients

For many automatic feature identification on the solar disk it is essential to make the background smooth. For this purpose, we first attempted a 2-D surface fitting. Even after this, we observed some non-uniformity still present in the images. Later we used a 1-D polynomial fitting to each row and column in the images. Care was taken that it does not produce any bias in the data but makes background more or less uniform as expected. It does not affect the study of properties of the solar features. We first fit a third degree polynomial to a one dimensional, row wise sliced pixels. The resulting fitted curve is subtracted from the original row wise sliced pixels by keeping
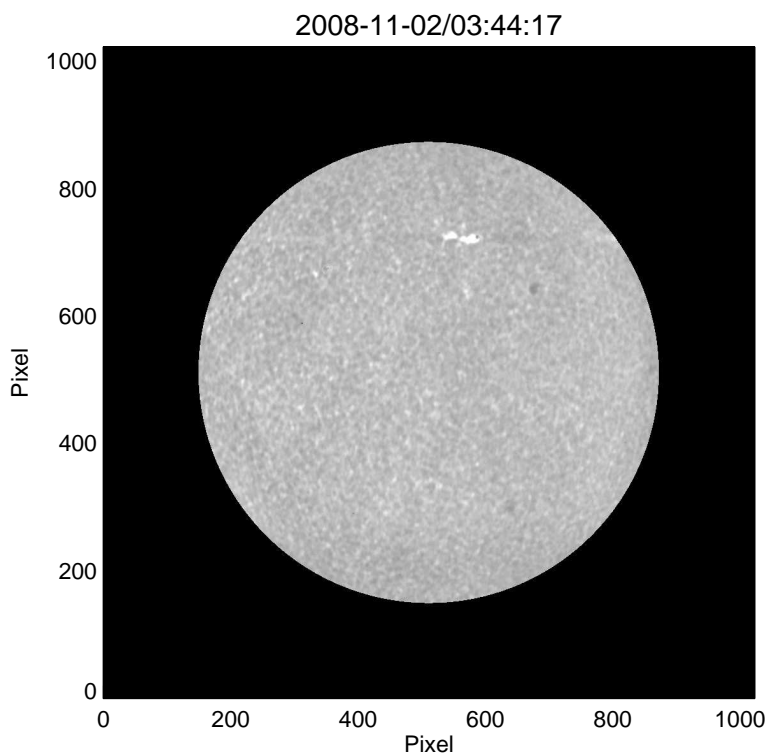
2008-11-02/03:44:17

Figure 4. Global fitted Ca-K image.

the mean level of the 1-D data as before. A similar fitting is done for column wise sliced pixels. Here too we used a third degree polynomial to remove the overall trend in the images. This procedure makes the background smooth and the resulting images (Fig. 4) show the network features with better contrast. Further details about this procedure can be seen in Singh et al. (2012).

4. Network element detection and area estimation

The synoptic data is essential to study the long-term variations in the plage and network element area index. To study the variations in area covered by these features it is essential to identify them automatically. One of the methods to identify the features is to use threshold values. The histogram of intensity values helps in deciding the threshold values. Fig. 5 shows the histogram of the intensity distribution in Ca-K images. The intensity values have been normalized to the background intensity. In the plot, the region between the first and second vertical lines represents the network. Similarly, the region between the second and third vertical lines represents the plage regions. The intensity before the first vertical line corresponds to the intra network regions. In a
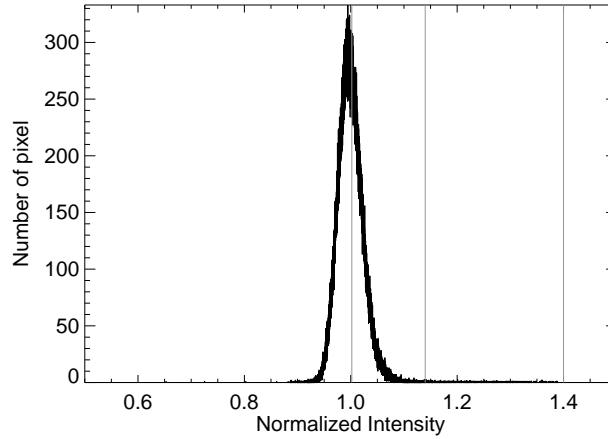
Figure 5. Histogram of the Ca-K image. The three vertical lines in the plot demarcates the intensity regions of intra network, network and plages.

distribution curve of various intensities in a Ca-K image, the peak value represents the mean value of the background intensity. If we normalize the whole image with respect to their mean value then the back-ground intensity value becomes about one. Then with respect to this normalized value the network elements and plages will have higher values.

4.1   Center to limb variation of network element contrast

Once the limb darkening correction is made and globally fitted to make the background uniform, the intensity contrast of the network elements become uniform from center to the limb. Fig. 6 shows the center to limb variation of the contrast values of the network elements. The intensity contrast has been estimated at each $\mu(=\cos\theta)$ value and averaged over a width of $\mu = 0.1$ and has been shown in the plot. The angle θ is computed from the center of the disk towards the edge of the disk. The value of angle θ is zero in the center and it is equal to $90°$ at the limb. We avoid the limb as the value of $\cos\theta$ ($=\mu$) will approach zero. The vertical bars represent the variations in the intensity contrast in a ring of $\mu = 0.1$. From the plot it is clear that the mean value of intensity contrast of the network elements is 1.02 and it varies from 1.006 to 1.035. Hence, the use of intensity threshold values with lower limit of 1.006 and upper limit of 1.04 should pickup all the network elements present on the disk. However in this study, we consider the enhanced network elements also as a part of the quiet network. The intensity contrast value of enhanced network is a little larger than 1.04 and we chose a upper threshold value of 1.14 to detect the quiet and enhanced network elements.
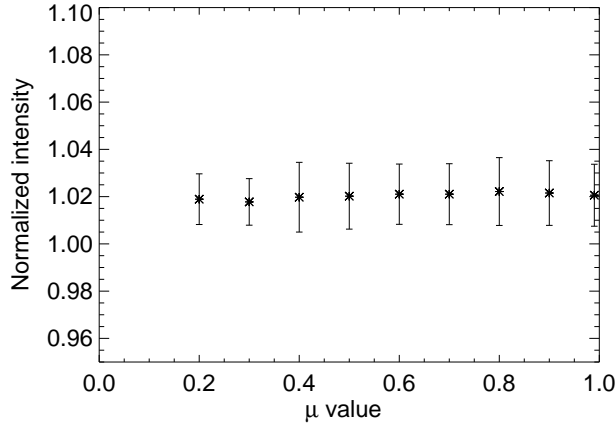
Figure 6. The intensity contrast of the network elements extracted from the region of ring with a width of μ=0.1. The vertical bars show the range of contrast values over the mean.

4.2 Thresholding and identification

Once the threshold has been decided quantitatively it is an easy task to examine how the values identify the network elements over the solar disk. In order to do that we overlaid the contours of the identified network elements based on the thresholds upon the processed image. For this purpose we used a small portion of the image of about 200×200 pixel around the disk center. Figs. 7 and 8 show the images extracted from the central portion of the Sun and overlaid with the contours of the identified network elements with various lower and upper threshold values. In Fig. 7 (top and middle rows) contours are obtained by varying the upper threshold values and keeping the lower threshold values at 1.002 above the background intensity level. The bottom row images show the contour levels that are obtained by varying the lower threshold levels while keeping the upper threshold levels fixed at 1.14 above the background value. The contours shown in Fig. 8 (top row) are obtained by varying the lower threshold values and by keeping the upper threshold values at 1.14 above the background level. In the bottom image the lower and upper threshold values are kept at 1.02 and 1.16, respectively, above the background value. From contour maps alone it is difficult to choose an optimum value of upper and lower threshold values. It is because most of the images show similar identification. Based on the contrast plot (Fig. 6) and many such contour images of different days we decided to choose 1.006 as the lower threshold and 1.14 as the upper threshold value. Once the network elements have been identified it is easy to isolate the plage regions. The intensity values above 1.14 isolate the plage regions. Fig. 9 shows the plage region identified using the threshold value of 1.14 above the background level.
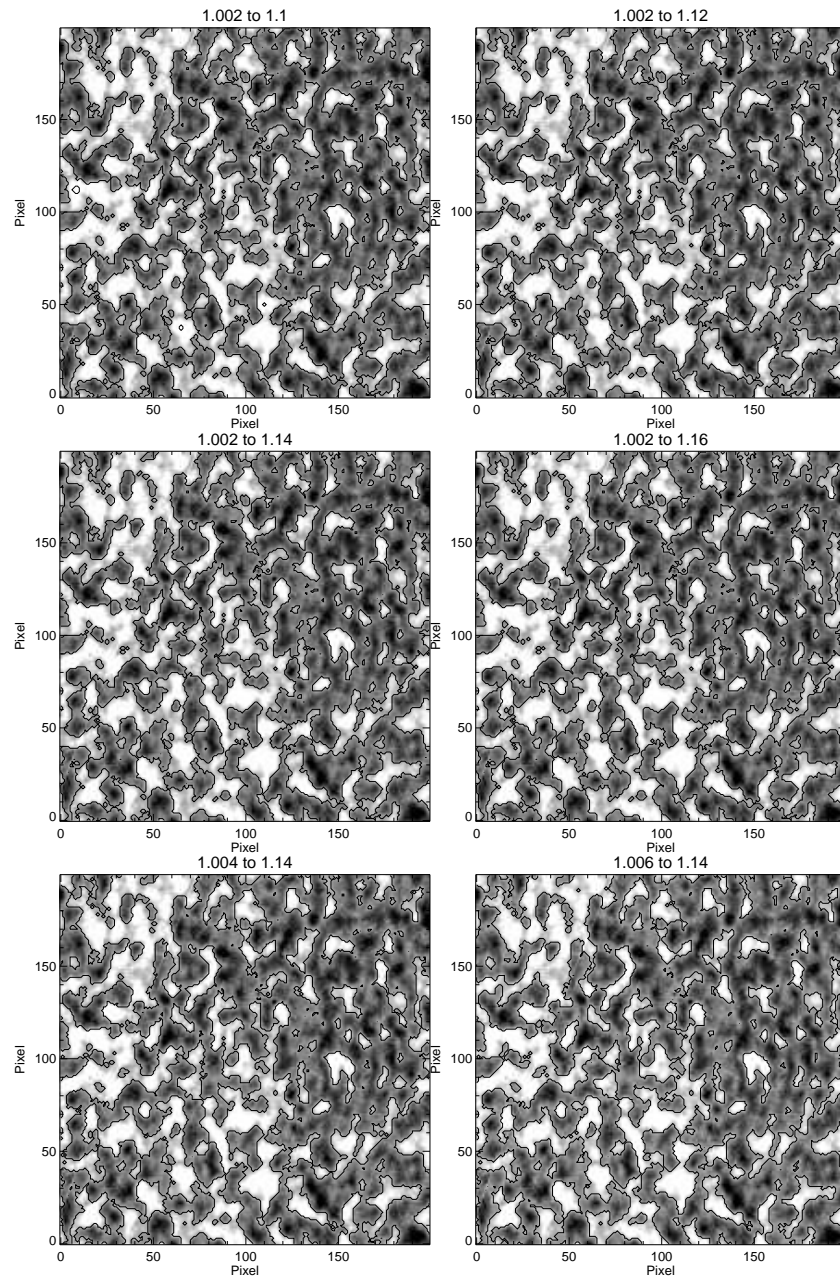
Figure 7. Contour map of detected network elements for different threshold values are overlaid upon the limb darkening removed image. The lower and upper threshold values of image contrast are shown on the top of each contour map.
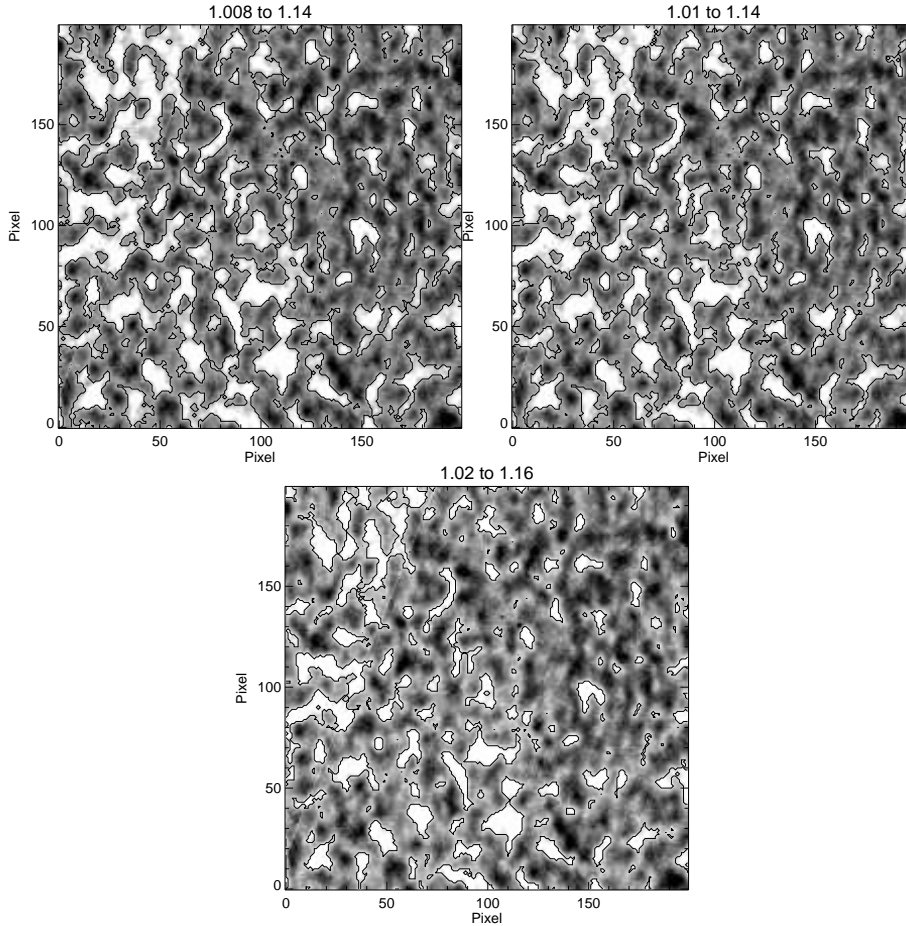
Figure 8. Same as Fig. 7, but for different values of threshold.

4.3 Network element area index

The network element area index estimates the area occupied by the network elements over the solar disk. It is expressed as a ratio of the area of the network elements occupied on the Sun to the area of the visible solar disk. Only the inner 90% of the solar disk is utilized in computing the network element area index. The remaining outer 10% of the disk is not used for the network element area calculation as the projection effect is quite large. We have computed the radius of the Sun for a particular epoch. The area occupied by all the pixels in contrast range from 1.006 to 1.14 was taken for network element area index calculation and the resulting network element area index is converted into percentage using the value of 90% of visible area of the solar disk as described above.
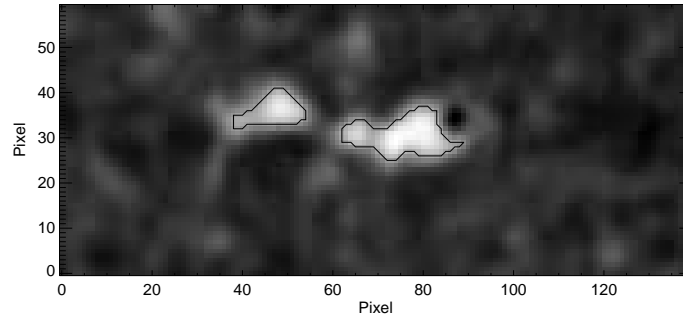
Figure 9. Contour of the plage region detected by the algorithm is overlaid upon the image enclosing the plage region.

The November 02, 2008 data set has a uniform cadence of Ca-K images and available for a long time period of about 5 hrs. Hence, we used the November 02 data here for the network element area index computation. Fig. 10(top) and (bottom) shows the network element and plage area index for the day of November 02, 2008. From the plot, it is clear that the network element area index varies over a day. This variation from morning to evening indicates that the determination of network element area index is sensitive to the seeing conditions. This is assuming the fact that the total network element area will not change over the disk within a few hours of observations. When the observation starts in the morning, normally the seeing conditions are good at Kodaikanal. The power to the Ca-K filter is switched ON when the observations start to avoid any damage to the filters in the night when no observer is at the telescope. The passband of the filter takes about 20 min to reach the central value. The lower Ca-K network element area index values in the beginning of the observations could be the result of small off band of the filter. It could also be due to the low altitude of the Sun in the early morning and hence large air column could be disturbing the contrast of the image. As the altitude of the Sun increases, the ground heating begins after 5:00 UT. This increases the atmospheric turbulence and hence seeing becomes poor with time. As this happens, the quality of the image degrades hence the network boundaries observed in Ca-K image become diffuse. This would cause the intensity of the network ///////elements below the threshold value of 1.006. Hence the poor seeing conditions affect the estimation of the area of network elements. The variation in the determination of network element area index due to seeing conditions is marginal at about 1-2% in the morning hours. The variation in the area index is moderately large in the noon when the seeing becomes poor by about 5″. From the plot it is clear that the network elements cover about 30% of the solar disk. On November 02, there was a small plage in the field-of-view and its area was about 0.07% of the visible solar disk. A small but noticeable decrease in its area was observed over the day. This could be due to the seeing variations or changes in the plage itself. A daily average of network element area index and plage area index for about 3 years (from February 2008 to February 2011) has been estimated and it is found that the network element occupied about 30% of the solar disk and the plage occupied less than 1% of the solar disk. It is also found that the network element area index decreases from February 2008 to February 2011 by about 7%. Further details about the result can be found in Singh et al. (2012).
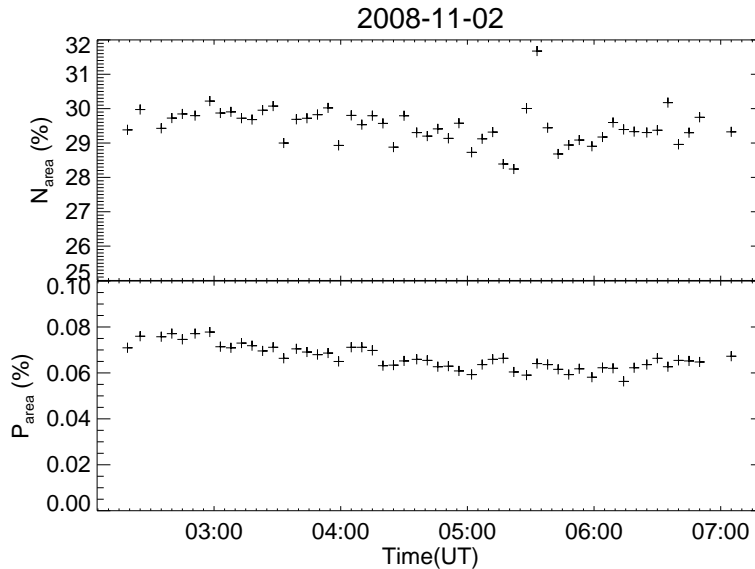
Figure 10. Network element area (top) and plage area (bottom) normalized to the Sun's visible area is plotted in terms of percentage for the data of November 02, 2008.

5. Summary

We have designed, developed and fabricated a Twin Telescope and installed at Kodaikanal Observatory. The instrument continues to provide data since February 2008 till date. This instrument is built to continue the Ca-K observations from Kodaikanal that has a history of 100 years of data obtained earlier in photographic plates. While the digitization of the historic data is going on, we have planned to develop some of the techniques to automatically identify various features observed in different wavelengths. We have applied an intensity threshold method for the processed Ca-K images obtained from Twin Telescope to identify the network elements and plages. Though, the method has some limitations, it is the first step in identifying the features. The main aim of the paper here is to announce the availability of a new telescope at Kodaikanal for the solar community and also to provide the information about the method of data calibration and reduction. In future, the calibrated data will be available to the researchers via the world wide web[1] interface of Indian Institute of Astrophysics. This provision will be made to provide the current day hourly updates on Ca-K images to the solar community. In future, the white light images for which the calibration process is currently underway, will also be made available to the solar community.

---

[1]http://kso.iiap.res.in:8080/KodaiTwinTelData/TwinTelCatalog.html

Acknowledgments

References

Denker C., Johannesson A., Marquette W., Goode P. R., Wang W., Zirin H., 1999, SoPh, 184, 87
Harvey K. L., White O. R, 1999, ApJ, 515, 812
HowardR. F., Sivaraman K. R., Gupta S. S., 2000, SoPh, 196, 333
Kuhn J. R., Lin H., Loranz D., 1991, PASP, 103, 1097
Makarov V. I., Sivaraman K. R., 1989, SoPh, 119, 35
MakarovV. I., TlatovA. G., SivaramanK. R., 2001, SoPh, 202, 11
Makarov V. I., Tlatov A. G., Sivaraman K. R., 2003, SoPh, 214, 41
Singh J., Bappu M. K. V., 1981, SoPh, 71, 161
Singh J., Prabhu T. P., 1985, SoPh, 97, 203
Singh J., Gupta S. S., 1995, SoPh, 158, 259
Singh J, Sakurai T., Ichimoto K., 2001, BASI, 29, 25
Singh J, Ravindra B., Selvendran R., Kumaravel, P., Priyal M., Priya T. G., Amareswari K., 2012, RAA, 12, 201
Sivaraman K. R., Gupta S. S., Howard R. F., 1999, SoPh, 189, 69
Sivaraman K. R., Gokhale M. H., Sivaraman H., Gupta S. S., HowardR. F., 2007, ApJ, 657, 592
Srivastava N., Mathew S. K., Louis R. E., Wiegelmann T., 2009, JGRA, 114, A03107